WATER MIST FIRE SUPPRESSION RESEARCH:
LABORATORY STUDIES

J. W. FLEMING[1], B.A. WILLIAMS[1], R.S. SHEINSON[1], W. YANG[2], and R.J. KEE[2]

SUMMARY

The water mist program at the U. S. Naval Research Laboratory (NRL) is an integrated effort for understanding water mist fire suppression, augmenting water mist effectiveness, observing water mist suppression in intermediate and large scale environments, and addressing implementation issues. This technology-based approach will lead to fire protection design guidance for military ship requirements, which are more challenging than many commercial needs. A crucial aspect of this program is the conduct of fundamental studies to quantify the behavior of water drops in well-characterized flames. Key to our understanding is the role of mist drop size in the flame suppression process. Equally important is information on the effect of various flame conditions, including flow field and temperature and their impact on the residence times of drops in the flame. This information is necessary in order to fully predict how drop parameters correlate with suppression effectiveness. Investigations with and development of multiphase models at the Colorado School of Mines (CSM) are allowing this predictive capability, permitting the treatment and understanding of the interplay of the drop behavior and flow fields. This paper presents experimental and modeling results on the effectiveness of water mist for fire suppression in premixed and in non-premixed counterflow flames with a particular emphasis on the effects of mist drop size.

1. INTRODUCTION

Research is needed to both identify and understand workable fire suppression strategies for fire threats currently protected by CF_3Br, Halon 1301. The likelihood of identifying a single replacement system is remote considering the diverse areas of application that must be protected. Application and replacement requirements including environmental demands and suppression effectiveness demand that replacement choices draw from a number of possibilities. Water mist is one of the technologies under consideration. Water mist fire suppression systems are currently used in some applications. Water mist is scheduled to protect machinery spaces on the next class of U. S. Navy ships. There is a strong desire to extend the areas of application to other areas of the ship and other platforms. Although water mist is very effective at fire suppression, it will not extinguish all fires as currently employed. Water could be used more efficiently, thereby extending the areas of application. However, the lack of a suitable technical base makes expanded usage problematic if not very risky. This paper addresses some of the technical aspects. The success of such programs, along with the attractive environmental properties exhibited by water, will provide workable replacement options for a greater number of applications than currently possible.

---

[1] *U. S. Naval Research Laboratory (NRL), Navy Technology Center for Safety and Survivability, Washington, DC 20375 USA; Email: fleming@code6185.nrl.navy.mil; phone: 202-767-2065; fax: 202-767-1716.*
[2] *Engineering Division, Colorado School of Mines, Golden, CO 80401 USA: Email: rjkee@mines.edu; phone: 303-273-3379; Fax: 303-273-3602.*

2. BACKGROUND

Water can be delivered to fires by several means, with various sized drops that demonstrate differences in behavior. Fire hoses deliver water in a relatively continuous stream, while sprinkler systems typically produce drops having diameters of a millimeter or more. Mist systems produce smaller drops, in the range of hundreds of micrometers for low pressure systems, and less than 100 micrometers for high pressure systems. Optimizing the use of water as a fire suppressant requires understanding the behavior of different sized water drops in the vicinity of flames of various geometries, as well as their transport from their source to the flame region. Additionally engineering issues must be considered; in general smaller drops are more difficult to produce, requiring more complicated and expensive generation equipment. It is known that drop size is important and that smaller drops are more effective. Thus one of the key questions is whether smaller drops have increased effectiveness sufficient to justify the trouble in producing them.

The water flow from a fire hose can pass through flames without efficient energy abstraction, often leading to flooding and water damage. Sprinklers are capable of delivering a more controlled amount of water in the form of smaller liquid drops. Current water-based fire suppression systems use far more water than should be required based on a comparison of water's sensible enthalpy to that of nitrogen or carbon dioxide. In fact, thermodynamic considerations predict that water should be as efficient as CF_3Br on a mass basis at suppressing combustion, provided the water can be efficiently transported to the fire and evaporate completely in the vicinity of the flame region. Water drops having diameters of less than 10 micrometers will likely evaporate completely for any flame geometry and residence time, but may evaporate too far from the fire to be effective. Since small drops have very little momentum, air currents, including those generated by the fire, can keep the small drops from reaching the fire. The transition from drops that follow the local gas flow field to those whose motion is dominated by momentum occurs at diameters on the order of a few micrometers. Quantitative information on drop size and vaporization in well characterized flow fields and flame geometries is needed to develop validated multiphase suppression models. These models can then be used as submodels in the prediction of water effectiveness against real fire scenarios. The studies outlined here address this need.

3. EXPERIMENTAL

3.1 Aerosol Generation

To study the effect of drop size on suppression properties, mists were generated using various methods. Submicron size drops (≤ 1 μm diameter) were generated using a venturi-based nebulizer (TSI Model 3076). A schematic of the nebulizer is shown in Figure 1a. Pressurized air, flowing through a small orifice, produces a high velocity air jet. The resulting pressure drop draws liquid from a reservoir through a small tube and entrains it in the air jet, breaking the liquid into drops. Larger drops impact the nebulizer wall and return to the reservoir. Drops small enough to remain entrained in the air flow are carried from the nebulizer. The amount of mist exiting the nebulizer was determined by measuring the change in mass of the liquid reservoir with time for a fixed air flow rate. Mists of polydisperse drops in the range of 1 to 20 μm were produced using another nebulizer (Airlife Nebulizer with Air Entrainment and Heater Adapter), a venturi-based nebulizer requiring an air flow of ~ 2.9 SLPM to generate drops.

Monodisperse drops of larger size ($\geq$ ~15 μm diameter) were generated using a vibrating orifice aerosol generator (VOAG, TSI Inc. Model 3450). A schematic of the drop generator is shown in Figure 1b. To generate the mist, liquid is forced through a pinhole using either a syringe pump or a plastic bag under pressure inside a small chamber. A limited amount of control over the liquid flow could be accomplished using either method. The size of the pinhole ultimately determined how much liquid could be delivered to the burner. The pinhole is acoustically excited by a piezoelectric ceramic driven at specific frequencies to break up the liquid jet into a stream of monodisperse drops. The drop size that could be produced depended on the pinhole diameter, the liquid flow rate, the forcing frequency, and the liquid properties. A dispersion cap was used to uniformly distribute the drop stream into a three dimensional mist although sacrificing some of the size monodispersity.

Drop size, velocity, and number density for the larger drops were measured using a phase Doppler particle anemometer (PDPA-Dantec Measurement Technology). For smaller drops ($\leq$ ~1 μm diameter), water concentration in the reactant stream was monitored by 90° scattering of a Helium-Neon laser at a wavelength of 0.6328 μm as

shown in Figure 2. The scattered laser light was detected with a photomultiplier tube (PMT) using a narrow-line optical filter. The laser beam was modulated at 1 kHz by passing the beam through a rotating slotted wheel. The laser beam was positioned just above the burner exit. A reference beam was split off just before the burner and monitored by a photodiode. The scattered and reference signals were processed with a lock-in amplifier (EG&G Instruments, Model 7265 DSP) and integrated over a period of 0.5 s. The scattering intensity was calibrated to a mist delivery rate by correlating the scattering signal with the change in water mass of the reservoir.

(a)   (b)
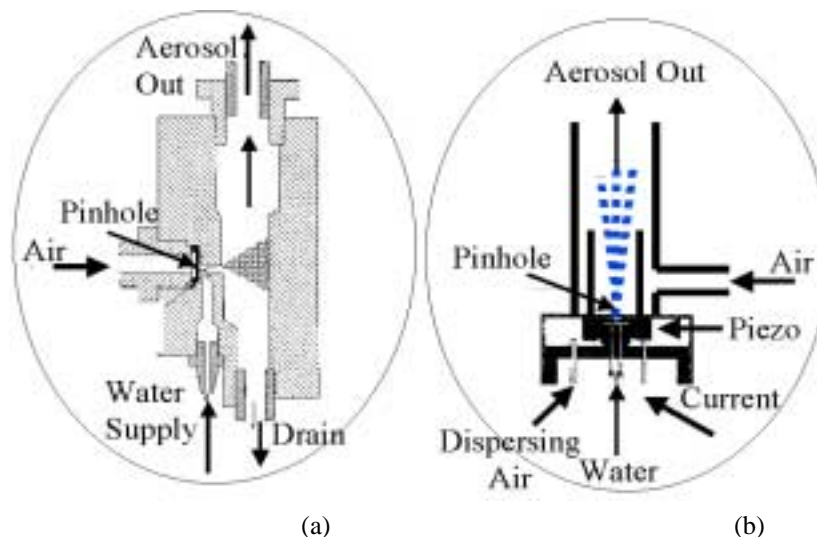
Figure 1: Schematic of water aerosol generation methods. (a) venturi-based atomizer for generation of sub-micron diameter water drops (TSI Inc., Model 3076). (b) vibrating orifice aerosol generator (VOAG, TSI Inc., Model 3450) for generating mono-disperse water drops > ~ 15 μm diameter.

3.2 Flame Configurations

3.2.1 Premixed Flames

The laminar burning velocity is a fundamental property of a flammable gas mixture and is frequently used as an indicator of the effectiveness of an inhibiting agent [Noto et al., 1996]. There are a variety of methods to measure laminar burning velocity [Andrews and Bradley, 1972]. We employed the total area method to quantify the reduction in burning velocity as a function of added mist in premixed conical flames. A schematic of the arrangement is shown in Figure 2. The burner is a converging nozzle with an exit diameter of 1.0 cm. An entrainment device to straighten the flow and uniformly seed drops in the gas flow utilized a perforated disk. The sub-micron size mist drops were small enough to pass through the ~ 0.16 cm diameter perforation holes. Larger drops ($\geq$ 5 micrometer diameter) were introduced through an opening in the middle of the perforated disk. The burner was enclosed inside a 13 cm diameter inner diameter acrylic tube that allowed optical access to the flame. The acrylic chamber was vented to an exhaust hood through a conical metal covering open at the top. A ~ 3 SLPM flow of nitrogen introduced through a sintered disk in the bottom of the chamber was used to purge the chamber of excess oxygen and product gases.

Video images of the flame were recorded to determine the burning surface area. Burning velocities for the inhibited flames are reported relative to the uninhibited burning velocity, thereby minimizing systematic errors in determining an absolute value for the burning velocity. Relative values derived from schlieren images for some of the flames are in good agreement with values derived from the visible flame surface. The presence of the aerosol reduces the flame burning velocity, which results in a taller flame with a larger flame surface area for a fixed fuel-air flow. To minimize any systematic effects due to varying flame height, fuel and air flows were adjusted to maintain a stoichiometric mixture and a flame height of 1.0 $\pm$ 0.15 cm. The measured burning velocities of nitrogen-inhibited flames were found to be insensitive to flame height over this range.
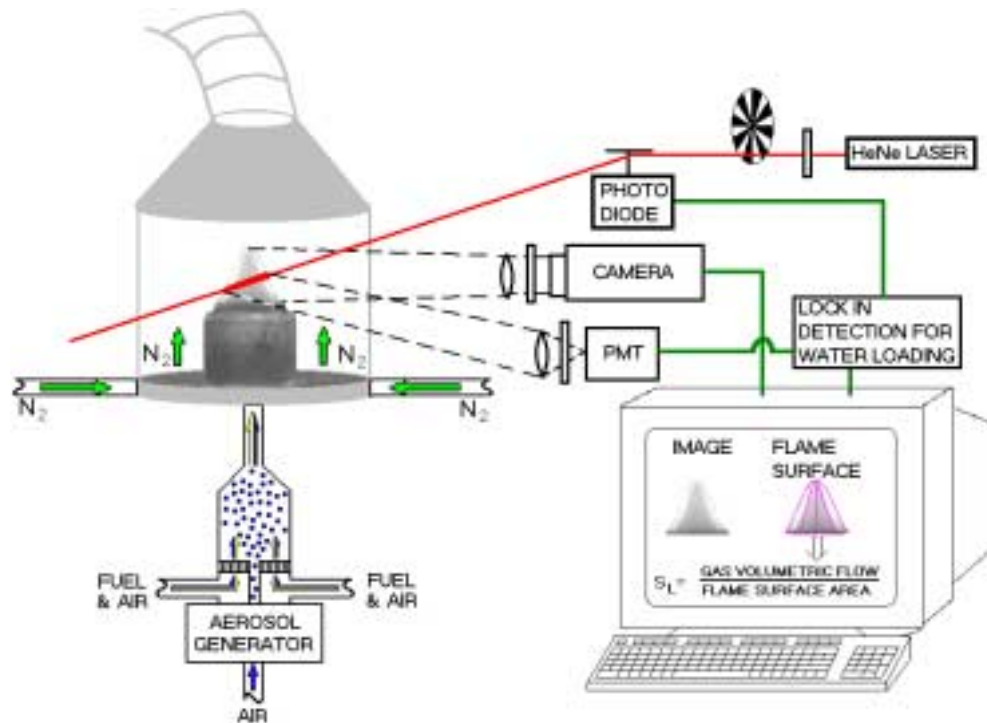
Figure 2: Schematic for the mist inhibited burning velocity determination in premixed flames. Water mist aerosols are seeded into the premixed gases. The flame is contained in an acrylic chamber, purged with a flow of nitrogen. Flame images are recorded using a CCD camera and a value for the total flame surface is determined. Burning velocities are determined by comparing the total flame surface to the volumetric flow of gases in the burner. Light from a modulated He-Ne laser, scattered from the aerosol in the premixed flow and detected with a lock-in detector, is used to determine the amount of water aerosol in the form of small drops introduced into the flame. PDPA is used to quantify the water concentration for mists of larger drops.

3.2.2 Non-Premixed Flames

Water mist suppression effectiveness in non-premixed flames was quantified by determining the extinction strain rate in counterflow flames. Details of the experiments are reported in [Zegers et al., 2000]. A schematic of the experimental configuration is shown in Figure 3. The burner consisted of two 50-cm long stainless steel tubes (1 cm inner diameter), with outer concentric tubes for a co-flow. The upper tube has a jacket for cooling water. The two tubes were aligned vertically and colinearly with a separation of 1.00 ± 0.05 cm. The end of the each tube was plumbed through a stainless steel plate on the top and bottom of a 22 cm inner diameter, 19 cm long acrylic tube. The acrylic tube has flat windows for good optical access. These windows are critical to both the position of the laser beam overlap for the PDPA measurements and the detection angle of the scattered light. A ~ 4 SLPM purge flow of nitrogen was introduced into the bottom of the chamber. All gases exited through the top plate of the combustion chamber through a 5 cm diameter exhaust port.
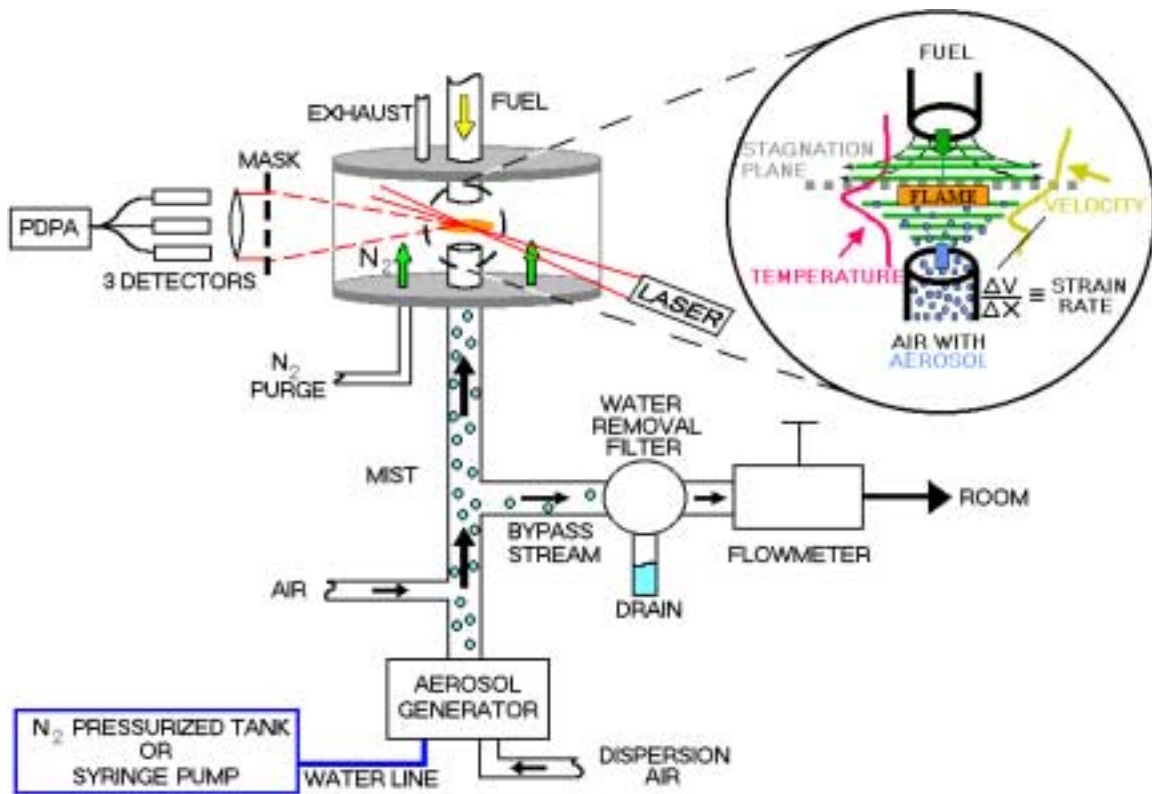
Figure 3: Schematic for water mist inhibited studies in non-premixed flames. Water mist aerosols are generated and seeded in the air flow in the lower tube. Fuel is introduced from the top, water-cooled tube. Flames are stabilized in a 1 cm gap between the two tubes. The burner is contained in an acrylic chamber, purged with a flow of nitrogen. The chamber has flat windows for optical access. Strain rates are determined from discrete velocity measurements using Laser Doppler Velocimetry. Phase Doppler Particle Anemometry is used to measure drop size, number density, and velocity through the flow field by vertically translating the burner assembly. The aerosol generator requires a ~1-1.5 SLPM flow of air for proper operation. In order to examine flames of lower strain rate, part of the air stream containing drops was diverted from the burner. Water drops from the excess stream were removed by filtering and the resulting air flow measured to determine the amount of air sent to the burner.

Flames were started using an impact arc igniter for a standard fuel and air flow configuration. For hydrocarbon fuels burning in air, stoichiometry dictates that the non-premixed flame reside on the air side of the stagnation plane. Mist was added with the air which typically was supplied from the bottom tube. Air size introduction of the mist is relevant to real fire, total flooding fire suppression scenarios. Representative centerline temperature and axial velocity profiles are indicated in Figure 3, as is the strain rate, the maximum gradient in the axial velocity on the air side of the flame. Experimental strain rates were evaluated using Laser-Doppler Velocimetry (LDV) by seeding the flows with ~ 0.35 μm diameter alumina particles or sub-micron water drops. In this flow field, stable flames can be maintained if a sufficient amount of heat and flame radicals generated from the combustion process can be conducted to the unreacted fuel and air as they flow into the reaction zone. Extinction occurs when the flow rate is too fast to maintain the flame. Under these conditions the flame strain rate exceeds a critical value referred to as the *extinction strain rate*. Suppression agents lower the extinction strain rate and this reduction is used to measure suppression effectiveness.

4. MODELING

The suppression effects of gas-phase agents were modeled using PREMIX [Kee et al., 1987] and OPPDIFF [Lutz et al., 1997]. The chemical reaction mechanism and the associated thermodynamic and transport properties were taken from GRI-Mech 3.0 [Smith et al., 2001] but with the nitrogen chemistry removed. The inhibition effects of water aerosols on premixed flames were calculated using a multiphase combustion model [Yang and Kee, 2002]. The multi-phase model solves conservation equations for mass, momentum, and energy for the water drops within a Lagrangian framework. One-dimensional conservation equations in an Eulerian framework are used to solve the physics of the gas-phase flame propagation. Coupling of the two phases is achieved through addition of drop-evaporation related source terms in the PREMIX software. Boundary conditions for the drop-evaporation dynamics are obtained from the PREMIX solution.

5. RESULTS AND DISCUSSION

5.1 Burning Velocity in Premixed Flames

The inhibition effect of sub-micron diameter water drops (nominal 0.35 μm) on the normalized burning velocity of a methane-air flame is plotted in Figure 4. Details of the experiment and results are reported in [Fuss et al., 2002]. Also shown are the inhibition effect of N_2, CF_4, and CF_3Br. The CF_3Br data are modeling results considering full chemistry [Noto et al., 1996; Parks et al., 1979]. On a mass basis, the inhibition effectiveness of water mist is comparable to that of CF_3Br.

A summary of an evaluation of the thermodynamic properties of the agents investigated in Figure 4 is listed in Table 1. Column 2 lists the sensible enthalpy per unit mass (per mole listed in column 3) required to raise the temperature of each agent from 300K to 1600K [Chase et al., 1985]. On a mass basis N_2 and CF_4 should contribute similarly to the inhibition. The sensible enthalpy for water mist, including the heat of vaporization at 1 atm, is roughly twice that of water vapor and 3.5 times higher than for N_2 or CF_4. Each of these predictions is consistent with the experimental observation. The mass of inhibitor required to reduce the burning velocity by 20% is listed in Column 4 and the molar amount in Column 5. The mass of liquid water needed to reduce the burning velocity by 20% is one third of that required for N_2 or CF_4, which is in good agreement with the thermodynamic estimate. The value for water is comparable to published measurements for CF_3Br. Thus, small water drops acting thermally exhibit a comparable effectiveness on a mass basis in premixed flames as CF_3Br with its chemical effect.

Both theoretical [Mitani, 1981; Blouquin and Joulin, 1998] and computational [Yang and Kee, 2002] models have been developed to predict premixed flame structure and extinction characteristics as a function of water-mist properties. Figure 5 illustrates the predicted dependence of the burning velocity on drop size and water loading. For small drops, the burning velocity decreases monotonically as a function of water loading. Also, for sufficiently small drops, the burning velocity becomes independent of drop size but still depends on water loading. For stoichiometric, methane-air, premixed flames, this small-drop limit is achieved for a drop diameter of approximately ten micrometers [Yang and Kee, 2002].

Experimental validation of the small-drop limiting behavior is presented in Figure 6. The sub-micron mist inhibition results are in excellent agreement with the model, requiring no adjustable parameters. Water vapor is both observed and predicted to be less effective than water aerosols of drop sizes less than ~ 15 μm. There is an increase in effectiveness of liquid water as the drop size is reduced down to ~ 10 μm. Below this size limit, there is no increase in suppression effectiveness with decreasing drop size. This limiting drop size correlates in the model with complete evaporation of the drops in this flow field.

Complete evaporation of the sub-micron mist drops by the time they enter the luminous flame zone was confirmed by monitoring light scattered from the drops in the flame using laser sheet illumination. Drop size measurements using PDPA for larger drops as a function of position in the flame are shown in Figure 7: size versus position in Figure 7a and number density versus position in the flame in Figure 7b. Drops ≥ 27 μm diameter were reasonably monodisperse (generated using the VOAG) and survive travel through this flame (peak temperature ~2100K, determined using a radiation-corrected, coated Pt/Pt-Rh thermocouple). The smaller drops generated with a nebulizer (average diameter 6 μm and $D_{v=0.9} < 10$ μm) completely evaporate at the flame front. Thus, the

experimental drop size for onset of complete evaporation in this flame is between 6 and 27 µm. These measurements are consistent with the predicted ~ 10 µm limiting drop size of the multi-phase model.
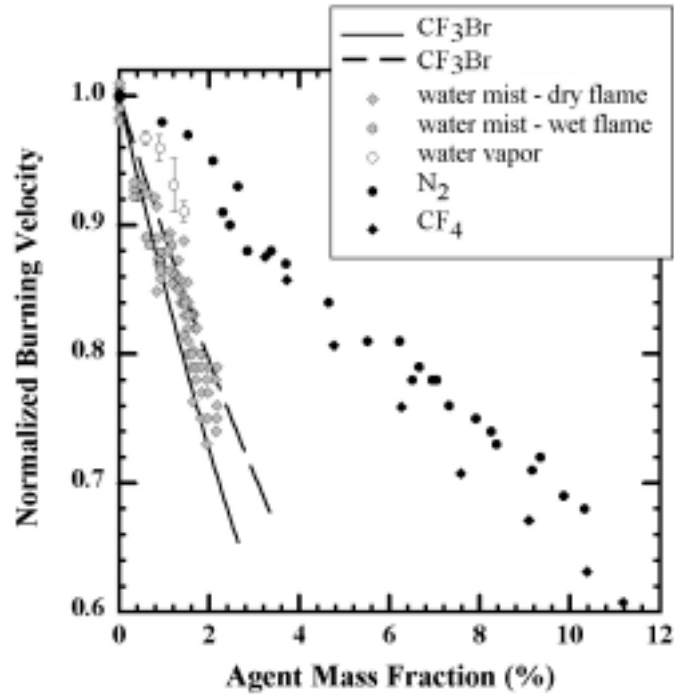
Figure 4: Normalized burning velocity reduction versus mass of added inhibitor: water in the form of sub-micron water drops in humidified flames (gray diamonds) and in un-humidified "dry" flames (gray circles), water vapor (open circles), N_2 (black circles), and CF_4 (black diamonds) [Fuss et al., 2002]. Results for CF_3Br are indicated by a dashed line [Parks et al., 1979] and a solid line [Noto et al., 1996].

Table 1: Relevant thermodynamic quantities and experimental suppression efficiencies for the thermal agents studied compared to CF_3Br. Columns 2 and 3 list the sensible enthalpy of each agent for a temperature range of 300K to 1600K. The value for water mist includes the heat of vaporization at one atmosphere. Columns 4 and 5 list the experimental mass and mole fractions of the total flow, respectively, required to reduce the uninhibited burning velocity by 20%. Uncertainties are derived from the standard deviations in the fits to the burning velocity reduction versus mass.

Agent	$(H_f^{1600K} - H_f^{300K})$ [a]		Mass Fraction	Mole Fraction
	kJ/g	kJ/mol		
N_2	1.5	42	6.3 ± 0.4	6.2 ± 0.4
CF_4	1.4	122	5.5 ± 0.4	1.9 ± 0.2
H_2O (vapor)	2.9	53	3.3 ± 0.2	5.0 ± 0.3
H_2O (mist)	5.2	93	1.7 ± 0.1	2.6 ± 0.2
CF_3Br	0.85	126	1.9 [b]	0.4 [b]

[a] Calculated from data in [Chase et al., 1985]
[b] Data from [Noto et al., 1998]
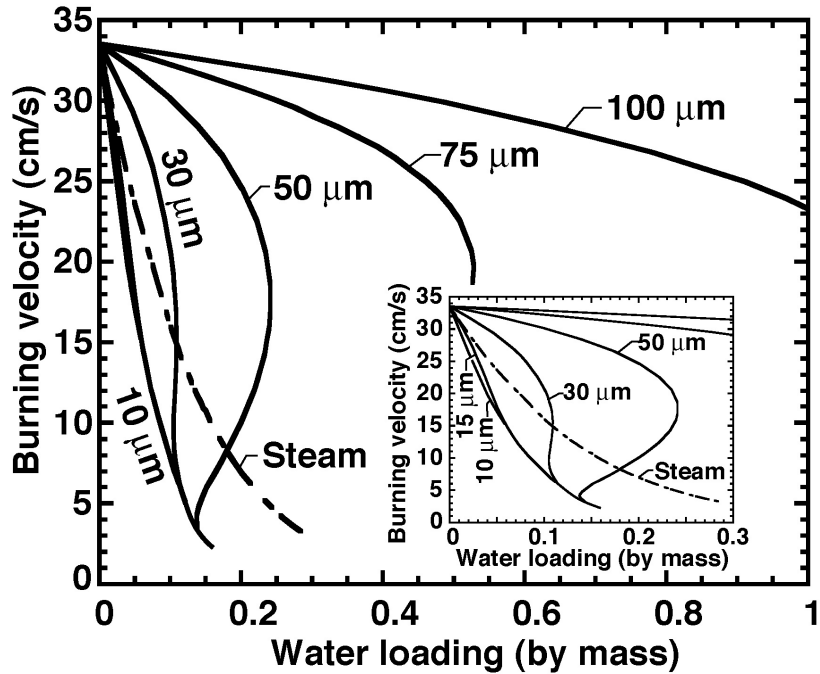
Figure 5: Predicted burning velocity for a stoichiometric, premixed, methane-air flame as a function of initial drop diameter and water mass loading [Yang and Kee, 2002].
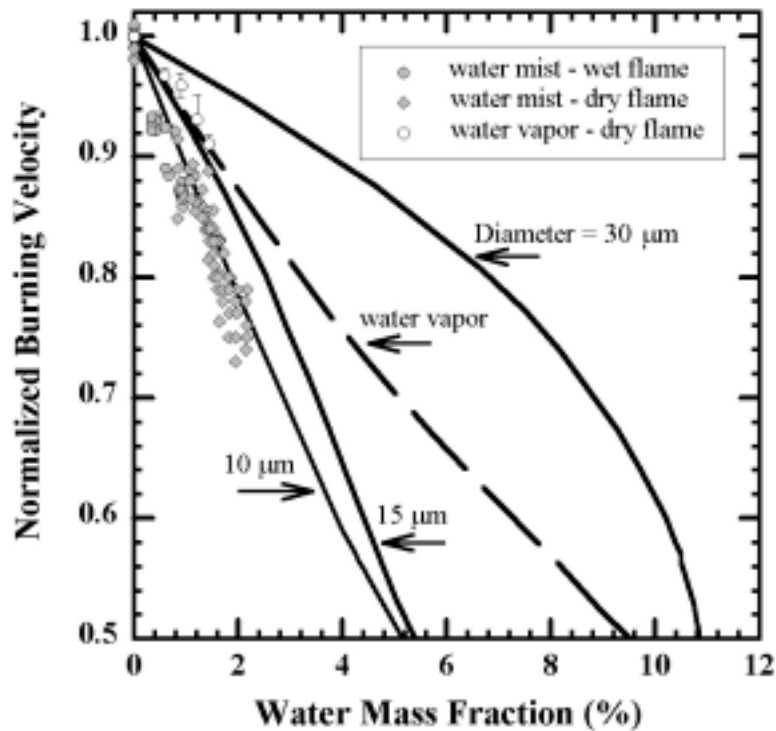
Figure 6: Normalized burning velocity for a water inhibited methane-air premixed flame showing the experimental results from Figure 7, and multi-phase flame modeling results for the indicated water drop sizes (solid lines) and PREMIX results for water vapor inhibited flame (dashed line) [Fuss et al., 2002].

Modeling predictions for the experimental conditions presented in Figure 7 are shown in Figure 8. Drop size versus position is shown in Figure 8a and relative drop number density versus position is shown in Figure 8b. Drop size behavior is in reasonable agreement in the post flame region. However, the experimental drop number density decay rates are much slower than the model predicts (note that the distance plotted in Figure 7b is four times that of Figure 8b.) The source of the difference can be attributed to the residence time of the drops in the flame. In the experiment, drops are traveling at the same speed as the gas phase, ~ 140 cm/s for these flames. In the one-dimensional freely propagating flame model, drops also travel at the same speed as the gas phase, ~ 30 cm/s. Thus, the prediction of a higher evaporation rate (shorter evaporation time) for the longer residence time in the model is consistent. Experiments to quantify the effect of larger drops on the burning velocity are pending.

(a)   (b)
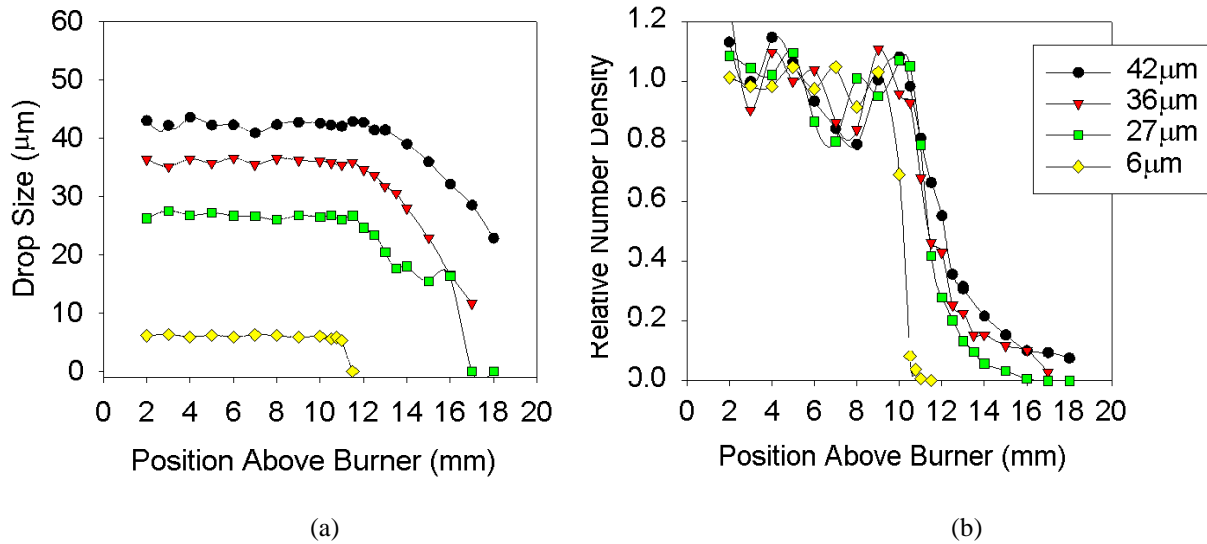
Figure 7: Experimental measurements of water drop behavior in a stoichiometric premixed methane-air flame as a function of height above the burner exit; (a) average drop size and (b) relative drop number density versus position for water aerosols of the indicated drop size. The relative burning velocity for the aerosol laden flames was ~ 90% that of the uninhibited flame.

(a)   (b)
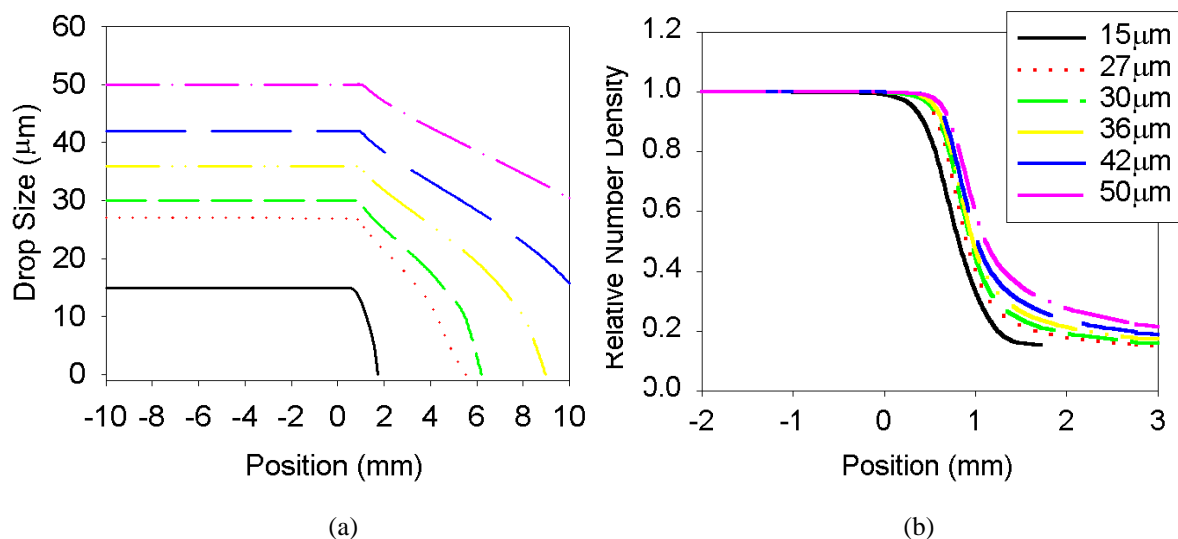
Figure 8: Multi-phase flame modeling predictions of water mist behavior in a stoichiometric premixed methane-air flame: (a) average drop size versus position in the flame and (b) relative number density versus position in the flame. The water mass fraction is 5%. The 0 mm position is the 300K left boundary for the freely propagating flame solution. Figures 7a and 8a are plotted over the same distance of 20 mm. The distance plotted in Figure 7b is four times that of Figure 8b.

The model predicts a turning-point behavior for the effect of moderate and larger sized drops (above 25 μm for stoichiometric, premixed, methane flames) on burning velocity as seen in Figure 5. At the turning point the derivative of burning velocity with respect to the water mass loading is infinite. Turning points are caused by the drop dynamics within the flame. Specifically, longer drop residence time in a suppressed flame causes further increase of efficiency in flame suppression. Mathematically, at a turning point, an infinitesimally small increase of water mass loading causes the burning velocity to fall to the lower branch of the suppression curve. Such very-low-burning-velocity branches are experimentally not achievable due to the various heat-loss mechanisms that would prevent these flames from stabilizing. Therefore, it may be safe to interpret such turning points as flame extinction points.

The theoretical and computational analyses predict that the burning-velocity curves join together in the lower-burning-velocity region. This behavior can be attributed to a greater drop residence time in the slow-burning flames. If the burning velocity is sufficiently low, any drop can totally evaporate within the flame, leading to equivalent efficiency for flame suppression.

The turning points predicted for larger drops can be important in fire suppression. Unfortunately, no direct observation or measurement of such behavior for inhibited premixed flames has been reported. The challenges to realizing such experiments include the generation of the mono-dispersed mists, the high water-mass loading required at turning points, and controlling the non-ideal conditions such as buoyancy and heat loss to the environment. Experiments that focus on the inhibition effects of larger drops are needed.

Understanding the inhibited flame structure and drop dynamics provides considerable insight into the mechanisms of flame suppression. The computational model predicts temperature, species concentration, number density, and drop history profiles throughout the flame. These variables represent the underlying factors that control the overall burning velocity. Therefore, detailed measurements of flame structure can be extraordinarily valuable. Unfortunately, both creating the flame and developing the required diagnostics are significant challenges. Figure 9 illustrates a comparison of the current models and experiments. Flame structure, burning velocity, and extinction characteristics are modeled as an ideal flat flame (Figure 9a). The experiment is represented by Figure 9b. The Bunsen-like configuration allows drops to be introduced through the open tube. The burning velocity in these flames is inferred from analysis of the flame area. In addition, flame profile data can be measured, for example on the centerline. However, data from such experiments cannot be compared directly to one-dimensional flat-flame models. The gas and drop velocities, for example, are much greater in the Bunsen-like flame. The sub-micron mist results, however, are certainly valid since the added water has all evaporated by the time it reaches the flame. It appears that there are two choices for modeling the inhibition effect of larger drops in premixed flames: configure a "flat" premixed, burner stabilized flame that can be seeded with large water drops, or directly model the three dimensional Bunsen-like flame. The success of uniformly seeding drops into a flat flame is highly unlikely considering the drop sizes to be studied. Success seems more likely for alternative modeling approaches.

(a)   (b)
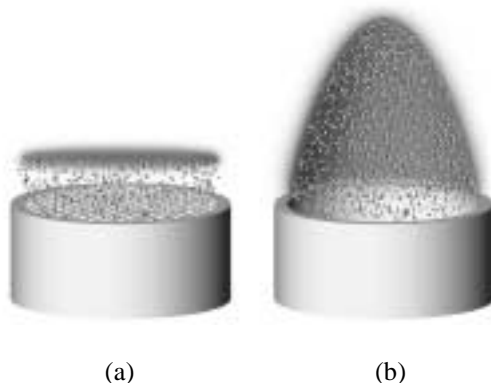
Figure 9: (a) Representation of an ideal mist inhibited flat flame as simulated in the modeling [Wang and Kee, 2002]. (b) Representation of the experimental inhibited premixed flames reported here.

It remains a challenge to create new models that better represent the experiments or to create new experiments that can be modeled more easily. On the modeling side, it should be possible to build channel-flow boundary-layer models that represent the Bunsen-like flame [Kee and Miller, 1978; Miller and Kee, 1977]. Such boundary-layer models are computationally efficient, indeed comparable in computational complexity with the flat-flame models [Raja et al., 2000]. However, the experiments must be configured in such a way as to render the boundary-layer models valid. The flow rates must be sufficiently high such that the axial convective transport is large compared to axial diffusive transport. Also, it may be necessary to pilot the flame, causing a well-defined stabilization mechanism. Since boundary-layer models neglect axial diffusion, they are not able to represent the physical stabilization mechanism on an ordinary Bunsen flame.

5.2 Extinction Strain Rate in Non-Premixed Flames

The effect of water mist on the extinction strain rate of non-premixed propane-air and methane-air counterflow flames was studied. Evaporation behavior of the aerosol drops in these flames was also determined. Experimental details and results are reported in [Zegers et al., 2000]. The water mass required for extinction of various strain rate flames is plotted in Figure 10. Also plotted is the amount of CF_3Br required for extinction. Water aerosols with a drop size of $\leq \sim 40$ µm are more effective than CF_3Br on a mass basis. Water drops that are 14 µm in diameter are ~ 3 times more effective than CF_3Br at extinguishing these flames. Phase Doppler Particle Anemometry was used to follow the drop size and number density throughout the flow field. We determined that water drops $< \sim 30$ µm diameter completely evaporate in these flames (mid to high strain rates). There is a large increase in effectiveness in going to smaller drop size as seen in Figure 10b. Experimental limitations prevented taking a full complement of data for 20 µm drops. Strain rate extinction concentration measurements that were taken for ~ 20 µm drops were found to be similar to the results for the 14 µm drops, suggesting a limiting drop size for effectiveness between 20 and 30 µm.

(a)   (b)
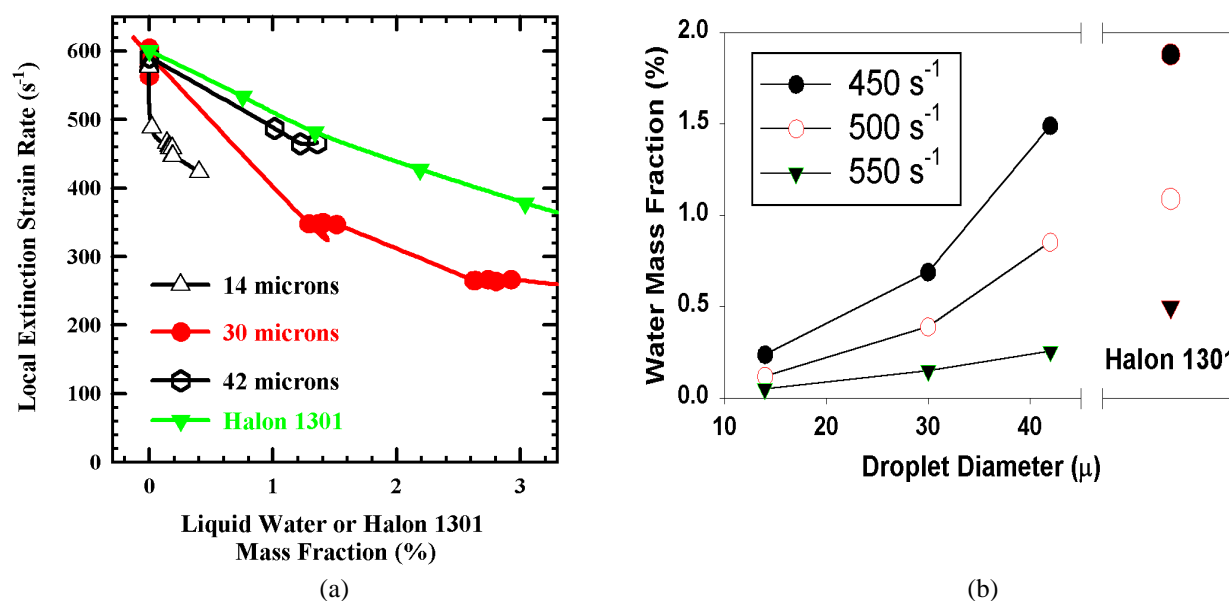
Figure 10: Water mist effects on the extinction of propane-air non-premixed counterflow flames. (a) Flame extinction strain rate as a function of mass of water or Halon 1301 (CF_3Br) in the air flow [Zegers et al., 2000]. (b) Mass of water to extinguish propane-air flames as a function of drop size, compared to gas-phase or Halon 1301.

Lentati et al., using a multi-phase flame suppression model they developed, predicted that 20 µm is the optimum size for effectiveness of water drops in these flames [Lentati and Chelliah, 1998a]. Our experimental observations are consistent with this prediction. A follow-up study using the same model reported an underprediction of a factor of two for the suppression effectiveness of a 20 µm water mist inhibited methane-air counterflow flame [Lazzarini et

al., 2000]. The difference could not be attributed to the non-monodisperse size distribution of the experimental mist. The counterflow flame model treats the drop trajectories in this flow field. Thus, the suppression difference is not likely due to drop residence times as is the case for the premixed flames. Although there is good qualitative agreement in observed and predicted water mist suppression properties in counterflow flames, further model validation is required.

5.3 Drop Evaporation Time Versus Flame Residence Time

5.3.1 Drop Evaporation Time

A key component to the suppression effectiveness of water mist is the enthalpy provided by the drop evaporation. Several models have been proposed for treating the evaporation of liquid drops, depending on what regimes are relevant and what assumptions are appropriate. One model suitable for water and the experimental conditions under consideration here is [Turns, 1996]:

$$D^2(t) = D_0{}^2 - K\,t \tag{1}$$

where K, the evaporation constant, is given by (2)

$$K = 8\,\lambda\,/\,(\rho\,c_p)\,\ln\,[1 + (T - T_{boil})(\,c_p\,/\,h_{vap})]$$

Suppression effectiveness is controlled by drop evaporation. The time for complete evaporation to occur can be estimated from:

$$t_{vap} = D_0{}^2\,/\,K \tag{3}$$

Equation 1 is referred to as the d-square law for drop evaporation and predicts the drop diameter, D, at any time, t, in terms of the original drop diameter, D_0. The mass transfer is dependent on the temperature, T, and thermal conductivity, λ, of the surrounding gas as well as on the properties of the drop: heat capacity at constant pressure, c_p; density, ρ; enthalpy of evaporation, h_{vap}; and boiling point, T_{boil}. According to Equation 3, the residence time required for the drop to completely evaporate is dependent on the original diameter of the drop. Evaporation times for water as a function of drop size for temperatures ranging from 1100 to 2200 K are shown in Figure 11. The evaporation time for a 30 μm diameter water drop in an air stream at 2100 K is seen to be ~ 2.5 ms.
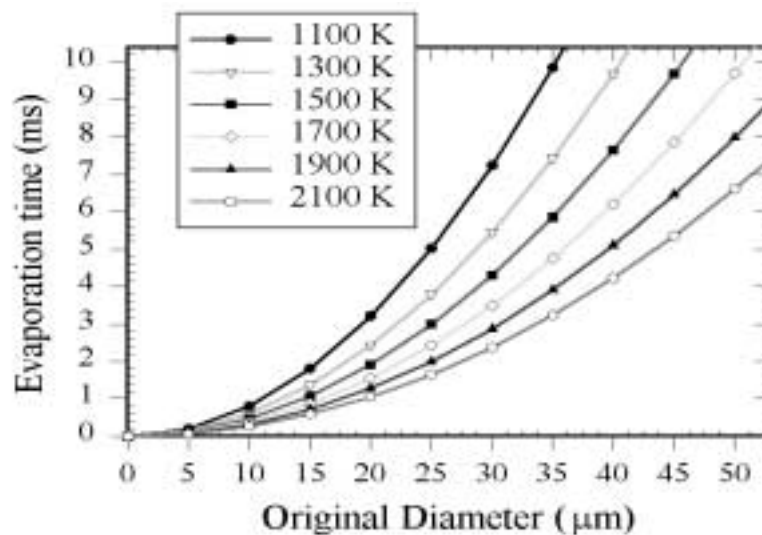
Figure 11: Predicted evaporation times using Equation 3 for water drops in air at the indicated temperature as a function of initial drop diameter. The thermal conductivity data for air is from [Kays and Crawford, 1980].

5.3.2 Drop Residence Time in the Flame

The degree of evaporation of water drops in the flame depends on the residence time of the aerosol in the high temperature environment. In the flame, the drop evaporation rate and drop size are spatially dependent since the aerosol is moving in a non-uniform temperature field. Solution of the problem requires full consideration of the flow field. However, the evaporation model can be used to estimate a drop size in the two flame configurations for the onset of complete drop evaporation. In the flame temperature field, drops begin to evaporate at the lower temperature and the resulting smaller drop, in traveling into the higher temperature region, will experience a higher evaporation rate and consequently a shorter total evaporation time.

Consideration of the burning velocity and flame thickness of the methane-air premixed flames studied here suggests that the water drops should experience a residence time in the range of 1-2 ms. Consideration of the temperature field and the results of Figure 11 indicate a drop size limit for complete evaporation (and the corresponding onset of drop limiting effectiveness) at ~ 15 μm in premixed flames. This upper limit estimate is consistent with the water drop size profiles observed in the premixed flame and with predictions of the multiphase model [Fuss et al., 2002].

For the propane-air and methane-air counterflow flames, transit time in the flame can be estimated from the inverse of the strain rate [Lentati and Chelliah, 1998]. For a strain rate of 450 s^{-1} (high strain rate for methane, mid strain rate for propane) the residence time is ~ 2.2 ms. The drop size for the onset of complete evaporation predicted from Figure 11 is ~ 25 μm. This value agrees with the experimental water drop size survival properties in propane-air flames [Zegers et al., 2002] and is consistent with the modeling predictions for methane-air flames [Lentati and Chelliah, 1998a].

The transition diameter from very effective small drops to larger, less effective drops depends on the evaporation rate of the aerosol. In general, evaporation times are shorter at higher temperatures. However, for premixed flames, higher flame temperatures mean higher burning velocities and shorter residence times. For counterflow flames, predicting drop evaporation for long residence times and large drops is complicated by several competing factors related to the inability of larger drops to follow the gas streamlines. For co-flow flames (e.g. in a cup burner) residence times are > 20 ms. In each of these flames there is a tradeoff between flame temperature, flow field, residence time and drop evaporation. Quantifying the inhibition effects of large drops is experimentally challenging since independent control of the two phases is difficult to accomplish. The interrelated dependencies on drop size and flame conditions explain why seemingly contradictory results have appeared in the literature quantifying the effectiveness of water mist.

5.4 Chemical Additives to Water Mist

Water mist, a physical agent, can be as or more effective than CF_3Br, consistent with the maximum sensible enthalpy that this condensed phase agent can provide to the flame though evaporation. There is the possibility of increasing the effectiveness of water through the use of a chemical additive. For the chemical additives, enhanced effectiveness is accomplished through the catalytic removal of H, OH, or O flame propagation radicals by the additive inhibitor species. Most of the potential additive compounds exist as liquids or solids at room temperature and many are water soluble to some extent. The effect of additional water on flames is almost entirely thermal [Seshadri, 1978] and water is already present in the flames as a combustion product. Thus water is unlikely to interfere with the chemical activity of these additives. In addition to the thermal benefit to fire suppression, water may be useful as a delivery method for non-volatile chemical fire suppressants

The enhanced suppression for water and additives comes about due to the synergistic effect of combining a chemical catalytic agent with water that acts through physical means. By lowering the flame temperature, water also lowers the concentration of the key flame propagation radicals, H, OH, and O. More importantly, the lower flame temperature results in an *increase* in the ratio of the concentration of these radicals to their thermal equilibrium concentration values, thereby making the catalytic cycles more favorable for further reducing the flame radicals.

Water mist additives that have been investigated include the alkali metal compounds. Zheng et al. reported the effect of 14 to 25 μm diameter aqueous NaOH drops on the burning velocity of premixed flames [Zheng et al., 1997]. We studied the burning velocity reduction in premixed methane-air flames by sub-micron size aqueous NaOH drops. Results for the extinction strain rate lowering in non-premixed methane-air counterflow flames by ~

20 μm diameter aqueous NaOH drops were reported [Lazzarini et al., 2000]. The ~ 20 μm drops in the non-premixed counterflow flames demonstrated an effectiveness for the combined effect of water and sodium consistent with predictions of evaporation time and flame residence time of the aerosol drops as well as the chemical contribution of the sodium. On the other hand, results for premixed flames depend heavily on the experimental conditions. *Either* essentially no effect for the water/additive aerosol above that of pure water is observed or there is abrupt flame extinguishment.

The alkali metal-water aerosol results are consistent with the characteristic residence times provided by the different flame configurations investigated and the drop size dictated evaporation times for water as discussed earlier. These studies point out that aerosol drop evaporation time (water plus additive) is even more important for the effectiveness of enhanced water mists than for pure water aerosols. In the case of additives with boiling points above ~ 100 ^{o}C, the water evaporation must be completed in time to allow the subsequent evaporation/decomposition of the residual particles and create the key chemical catalytic player that will participate in the chemical suppression cycle. Water drops that are just small enough to completely evaporate just as they leave the flame zone will likely be too large to be able to release the chemical additive in time to participate optimally in the suppression process. Quantitative determination of the suppression effectiveness of water mists with additives must be deconvoluted from the properties of the aerosol introduced into the flame, including size and thermodynamic properties (e.g. boiling/decomposition temperature and heat capacity), and the properties of the flame (including temperature field and flow field configuration).

One benefit of the presence of additives to water mist may lie in the creation of solid particle residue. Extinction strain rate lowering of methane-air non-premixed counterflow flames by aqueous aerosols of both liquid and solid phosphorus compounds have been recently reported [Jayaweera et al., 2002]. They observed that additives that left a particle residue were slightly more effective than phosphorus compounds that left no residue. Differences in the chemical composition of the additive compounds were considered and may play a small role. However, the increased effectiveness may be due to the presence of the particles themselves. In addition to the increase in the total sensible enthalpy due to the decomposition or evaporation of the particles, the particles could also increase the heat loss from the flame via radiation or increased heat conduction. These mechanisms have been predicted for inert particles in flames [Ju and Law, 2000; Blouquin and Joulin, 1998]. The experimental studies show that although the physical effect of residual particles formed from the aerosols on the flame leads to an enhanced suppression effectiveness, participation of phosphorus in the gas-phase chemistry is the primary suppression mechanism. However, the reaction mechanism for phosphorus inhibition requires more work before the role of the particles can be fully explored.

6. CONCLUSIONS

We have investigated the flame suppression effectiveness of water mist as a function of drop size in both premixed Bunsen-like flames and non-premixed counterflow flames. The evaporation behavior of individual drops correlates with the measured suppression effectiveness in premixed flames (flame burning velocity reduction) as well as in non-premixed flames (extinction strain rate lowering). Measurements show that water mist under the appropriate conditions can be as effective as CF$_3$Br on a mass basis at inhibiting flames. These results are consistent with an evaluation of the thermodynamic properties indicating that the thermal capacity of water mist can be used effectively in comparison with gaseous thermal agents, given suitable conditions. Water mist inhibited burning velocity measurements are also in excellent agreement with modeling predictions incorporating detailed combustion chemistry and multicomponent molecular transport. The model predicts the mass of water required to inhibit the flames decreases with decreasing drop size, reaching a limit at small drop size, below which there is no further suppression advantage based on mass of water added. The drop size limit that assures complete evaporation provides the maximum suppression effectiveness per mass of added aerosol. Drop residence time in the elevated temperature of the flame flow field is key to the suppression performance as it controls the extent of water evaporation.

The conclusions presented in this paper, based on the suppression behavior of water mist in laboratory flames, also provide understanding for water mist based systems. Understanding both drop size and transport behavior is critical to making quantitative predictions for water mist behavior. The results presented here contribute to that understanding and provide data necessary for the further development of models to predict water mist suppression in real fire scenarios.

7. ACKNOWLEDGMENTS

8. REFERENCES

Andrews, G. E., and Bradley, D. (1972), "Determination of Burning Velocities-Critical Review," *Combust. Flame* **18**, pp 133-153.

Blouquin, R. and Joulin, G. (1998), "On the Quenching of Premixed Flames by Water Sprays: Influences of Radiation and Polydispersity" , *Proc. Combust. Inst.*, **27**, pp 2829-2837.

Chase Jr., M. W., Davies, C. A., Downey Jr., J. R., Frurip, D. J., McDonald, R. A., and Syverud, A. N. (1985), *Journal of Physical and Chemical Reference Data* 14, Supplement 1.

Fuss, S.P., Chen, E.F., Yang, W., Kee, R.J., Williams, W.A, and Fleming, J.W. (2002), "Inhibition of Premixed Methane-Air Flames by Water Mist," *Proc. Combust. Inst.* **29**, accepted.

Jayaweera T. M. and Fisher* E. M., and Fleming, J.W. (2002), "Flame Suppression By Aqueous Solutions Containing Phosphorus", *Combust. Flame* , accepted.

Ju, Y. and Law, C.K. (2002), "Dynamics and Extinction of Non-Adiabatic Particle-Laden Premixed Flames," *Proc. Combust. Inst.* **28**, pp 2913-2920.

Kays, W.M. and Crawford, M.E. (1980), *Convective Heat and Mass Transfer*, 2nd ed., McGraw-Hill Book Company, New York, p 388.

Kee, R.J. and Miller, J.A., (1978), "A Split-Operator, Finite-Difference Solution for Axisymmetric Laminar-Jet Diffusion Flames", *AIAA J.*, **16(2)**, pp 169-176.

Kee, R.J., Grcar, J.F., Smooke, M.D., and Miller, J.A., (1987), A Fortran Program for Modeling Steady Laminar One-Dimensional Premixed Flames, Sandia National Laboratories, SAND85-8240.

M.D. Lazzarini, A.K., Krauss, R.H., Chelliah, H.K., and Linteris, G.T. (2000), "Extinction Conditions of Non-Premixed Flames with Fine Droplets of Water and Water/NaOH Solutions," *Proc. Combust. Inst.* **28**, pp 2939-2945.

Lentati, A.M. and Chelliah, H.K. (1998), "Dynamics of Water Droplets in a Counterflow Field and Their Effect on Flame Extinction," *Combust. Flame* **115**, pp 158-179.

Lentati, A.M. and Chelliah, H.K. (1998a), "Physical, Thermal, and Chemical Effects of Fine-Water Droplets in Extinguishing Counterflow Diffusion Flames", *Proc. Combust. Inst.* **27**, pp 2839-2846.

Lutz, A.E., Kee, R.J., Grcar, F.M. and Rupley, F.M., (1997), *OPPDIF: A Fortran Program for Computing Opposed-Flow Diffusion Flames*, Sandia National Laboratories, SAND96-8243.

Miller J.A. and Kee, R.J., (1977), "Chemical Nonequilibrium Effects in Hydrogen-Air Laminar Jet Diffusion Flames", *J. Phys. Chem.*, **81**, pp 2534-2542.

Noto, T., Babushok, V, Burgess Jr., D. R., Hamins, A., Tsang, W., and Miziolek, A. (1996), "Effect of Halogenated Flame Inhibitors on C_1-C_2 Organic Flames," *Proc. Combust. Inst.,* **26**, pp 1377-1383.

Noto, T., Babushok, V., Hamins, A., and Tsang, W. (1998), "Inhibition Effectiveness of Halogenated Compounds," *Combust. Flame* **112**, pp 147-160.

Parks, D. J., Alvares, N, J., and Beason, D. G. (1979), "Fundamental Flame-Speed Measurements in Combustion Gases Containing CF_3BR," *Fire Safety J.* **2**, pp 237-242.

Raja, L.L., Kee, R.J., Deutschmann, J.W. and Schmidt, L.D., (2000), " A Critical Evaluation of Navier-Stokes, Boundary-Layer, and Plug-Flow Models of the Flow and Chemistry in a Catalytic-Combustion Monolith, " *Catalysis Today*, **59**, pp 47-60.

Seshadri, K. (1978), "Structure and Extinction of Laminar Diffusion Flames Above Condensed Fuels with Water and Nitrogen," *Combust. Flame* **33**, pp 197-215.

Smith, G.P., Golden, D.M., Frenklach, M., Moriarty, N.W., Eiteneer, B., Mikhail Goldenberg, M., Bowman, C.T., Hanson, R.K., Song, S., Gardiner, Jr., W.C., Lissianski, V.V., and Qin, Z. (2001), *GRI-Mech 3.0*, http://www.me.berkeley.edu/gri_mech/.

Turns, S. (1996), *An Introduction to Combustion: Concepts and Applications*, 1st ed., McGraw Hill, Inc, New York, p 314.

Yang, W. and Kee, R.J. (2002), "The Effect of Monodispersed Water Mists on the Structure, Burning Velocity, and Extinction Behavior of Freely Propagating, Stoichiometric, Premixed, Methane-Air Flames," accepted *Combust. Flame*.

Zegers, E.J.P, Williams, B.A., Sheinson, R.S., and Fleming, J.W. (2002), "Dynamics and Suppression Effectiveness of Monodisperse Water Droplets in Non-Premixed Counterflow Flames," *Proc. Combust. Inst.* 28, pp 2931-2938.

Zheng, R., Bray, K.N.C., and Rogg, B. (1997), "Effect of Sprays of Water and NaCl-Water Solution on the Extinction of Laminar Premixed Methane-Air Counterflow Flames," Combust. Sci. Tech. **126**, pp 389-401.